Jurnal Penelitian Fisika dan Aplikasinya (JPFA)
Volume 12, Issue 2, December 2022
https://journal.unesa.ac.id/index.php/jpfa/

p-ISSN: 2087-9946
e-ISSN: 2477-1775

The Effect of Couple Doping Gd and Co on The Physical Characteristics of $LaFeO_3$ Thick Film for Acetone Gas Sensor Application

Hendi Haryadi [1,a], Dani Gustaman Syarif [2,b], and Endi Suhendi [1,c,*]

[1] Program Studi Fisika, Universitas Pendidikan Indonesia
Jalan Dr. Setiabudi No. 229, Bandung 40154, Indonesia
[2] Badan Riset dan Inovasi Nasional
Jalan Tamansari No. 71, Bandung 40132, Indonesia

e-mail: [a] hndhryd@upi.edu, [b] danigus@batan.go.id, and [c] endis@upi.edu
* Corresponding Author

Received: 18 October 2022; Revised: 11 November 2022; Accepted: 30 December 2022

Abstract

The acetone gas sensor is one type of sensor being researched for its application because it detects the presence of diabetes in sufferers. Gas sensors with high sensitivity and low operating temperature have been extensively investigated for this purpose, and this research is focused on the same purpose. Synthetization and characterization of $LaFeO_3$ with co-doping Gd_2O_3 and CoO thick film ceramics for acetone gas sensor was conducted. $LaFeO_3$ was made using the co-precipitation method with 2.5% CoO for each and 0%, 2.5%, and 5% Gd_2O_3 variation to the $LaFeO_3$. The $LaFeO_3$ thick film was prepared using the screen-printing technique and calcined at 800°C for two hours. The analysis of crystal structure characterization using X-Ray Diffraction (XRD) resulted in $LaFeO_3$ with co-doping Gd_2O_3 and CoO thick film ceramics having the same cubic crystal phase with smaller lattice parameters and crystallite sizes after doping were added. The results of morphology structure characterization using Scanning Electron Microscopy (SEM) showed the grain size of the $LaFeO_3$ with co-doping 2.5% CoO and 0%, 2.5%, and 5% Gd_2O_3 samples to support the analysis of electric property characterization later on. The electric property characterization showed that $LaFeO_3$ with various Gd_2O_3 concentrations, as part of co-doping with 2.5% CoO, resulted in higher sensitivity compared to the lacking of Gd_2O_3 one. In order, the maximum sensitivity values of each Gd_2O_3 concentration are 2.74, 3.06, and 8.76 when exposed to 270 ppm acetone gas at 310°C. Gd_2O_3, as part of co-doping in $LaFeO_3$ with CoO 2.5%, has successfully increased the sensitivity to the gas sensor yet still can not meet the expectation towards the operating temperature, which is still high compared to other references.

Keywords: *$LaFeO_3$; Gd_2O_3; CoO; Thick Film; Acetone Gas Sensor*

How to cite: Haryadi H, et al. The Effect of Couple Doping Gd and Co on The Physical Characteristics of $LaFeO_3$ Thick Film for Acetone Gas Sensor Application. *Jurnal Penelitian Fisika dan Aplikasinya (JPFA)*. 2022; **12**(2): 115-126.

INTRODUCTION

DOI: 10.26740/jpfa.v12n2.p115-126

The gas sensor is a sensor that is used to detect and identify the presence of gas in an area [1]. The acetone gas sensor is one type of sensor being researched for its application to detect the presence of diabetes in sufferers [2]. In general, the materials used for manufacturing gas sensors are oxide semiconductors and metal oxides [3]. Some examples of materials used include SnO_2 [4], TiO_2 [5], Fe_2O_3 [6], $LaFeO_3$ [7], and so forth [8].

$LaFeO_3$ is one of the constituent materials of gas sensors, which is sensitive to certain gases [9-11]. However, to be able to detect the presence of gas in a large range, it is necessary to engineer the material by doping [12]. The doping carried out by Chen et al. on $La_{1-x}Pb_xFeO_3$ (x = 0.0-0.5) has a sensitivity of 7 for 50 ppm acetone gas [13]. Pb doping causes the average grain size to be smaller, and the effect on the surface to volume ratio becomes larger so that the gas sensor performance increases [13,14]. Hao et al. also doped Ni on $LaFeO_3$, so a sensitivity of 82.75 was obtained for 100 ppm acetone gas [15]. Smaller grain size after doping increases the sensitivity of the gas sensor [12,16]. However, the operating temperature of the gas sensor is still relatively high for the two previous studies, which are 240°C [13] and 220°C [15], respectively.

Co-doping is the distribution of two dopants, each of which is a different element, to improve the performance of its electronic properties [17]. Gd was chosen as one of the dopants because several studies showed that Gd as a dopant increased the sensitivity in terms of the structure after being doped [18] with low concentrations for gas sensor applications [19,20]. In addition, Gd also provides a lower operating temperature than the two previous studies, namely 200°C for acetone gas [18]. The element Co was chosen as the Gd dopant partner in the co-doping of this study because a study using CoO has shown good performance in detecting the presence of acetone gas with high sensitivity [21]. Couple doping has shown promising results in terms of enhancing material properties, especially in lowering operating temperature and gas detection sensitivity, which is proven by Zeany et al. focusing on $LaFeO_3$ couple doped with ZnO and CaO [22].

With that knowledge to enhance sensitivity and lower operating temperature, this study's objective would focus on manufacturing acetone $LaFeO_3$ gas sensors with Gd and Co dopant in couple doping (co-doping), hoping to achieve both aspects.

METHOD

Preparation of $LaFeO_3$ co-doping Gd and Co Powders

In this study, three samples of $LaFeO_3$ were being couple-doped with Gd_2O_3 as much as 0%, 2.5%, and 5% mole percent, along with CoO for each sample of 2.5% mole percent on La_2O_3, Fe_2O_3, Gd_2O_3, and CoO powder were being made using co-precipitation technique. Each powder was dissolved in 12 M HCl and mixed to form a mixture of $LaFeO_3$ co-doping Gd and Co. The mixture was precipitated using ammonia hydroxide and then filtered and dried at 100°C for 6 hours and calcined in a furnace for 3 hours at 800°C.

Thick Film Fabrication

The calcined material, which is already in powder form, is made in the form of a thick film using the screen-printing technique. Each powder is mixed with an organic vehicle (OV) with a composition ratio of 70% OV and 30% powder to form a paste. The paste was coated on an alumina substrate that had been coated with silver and burned at 800^0C for two hours.

Thick Film Characterization

Structural characterization was done using X-Ray Diffraction (XRD) Rigaku Smart Lab for crystallography in Institut Teknologi Bandung's Hydrogeology and Hydrogeochemistry Laboratory with 2theta (2θ) ranging from 20° to 80° and Scanning Electron Microscopy (SEM) JSM-6510A type with the sample needs to be dry with 1 cm diameter and 5mm thick in maximum. XRD was carried out to see the crystal structure of thick film ceramics, and the results were analyzed using *Match!3,* so the crystal phase, crystal plane orientation (miller index, hkl), lattice parameters (a, b, and c) and crystallite size (D) were obtained. The crystallite size was obtained from the Debye-Scherrer Equation [23], which is shown in Equation (1), namely

$$D = \frac{0.9\lambda}{B\cos\theta} \tag{1}$$

SEM was carried out to see the morphological structure of thick film ceramics. The results were analyzed by comparing the resulting image scale with the standard magnification scale to obtain the grain size.

Characterization of the electrical properties was conducted to see changes in the gas sensor when exposed to acetone gas, which was indicated by changes in resistance and sensitivity. This characterization was carried out using a gas chamber tool set. The electrical characterization test was carried out by measuring the resistance of the sample to temperatures up to 315°C by recording data for every 5°C change, both in ambient conditions and when acetone gas was given with varying concentrations, starting from 90 ppm, 180 ppm, and 270 ppm. The data from the resistance test results are in the form of the resistance value and the temperature when the resistance is read. The data is then plotted against temperature to see changes in resistance and then see how sensitive it is. The sensitivity value is obtained from Equation (2) [24].

$$S = \frac{(R_g - R_a)}{R_a} \tag{2}$$

RESULTS AND DISCUSSION

Crystal Structure Characteristic

The results of the crystal structure characterization in the form of XRD test are presented in the form of a graph of the diffraction pattern shown in Figure 1. The $LaFeO_3$ diffraction pattern appears to have formed along with $Fe2O_3$ and alumina substrate, based on the comparison with the reference database from the Crystallography Open Database no. 96-154-2033 [25]. The crystal phase formed for the three samples has the same phase, namely a $P\bar{m}3m$ cubic crystal phase with miller index in sequential order (100), (110), (111), (200), (210), (211), (220), and (310). The lattice parameters were obtained using the relation between Bragg's law and $h^2 + k^2 + l^2$'s cubic structure. $LaFeO_3$ with co-doping Co 2.5% with Gd 0% has the value of $a = b = c =$ 3.9301 Å, for Gd 2.5% it is $a = b = c = 3.9284$ Å, and for Gd 5%, it is $a = b = c = 3.9274$ Å.

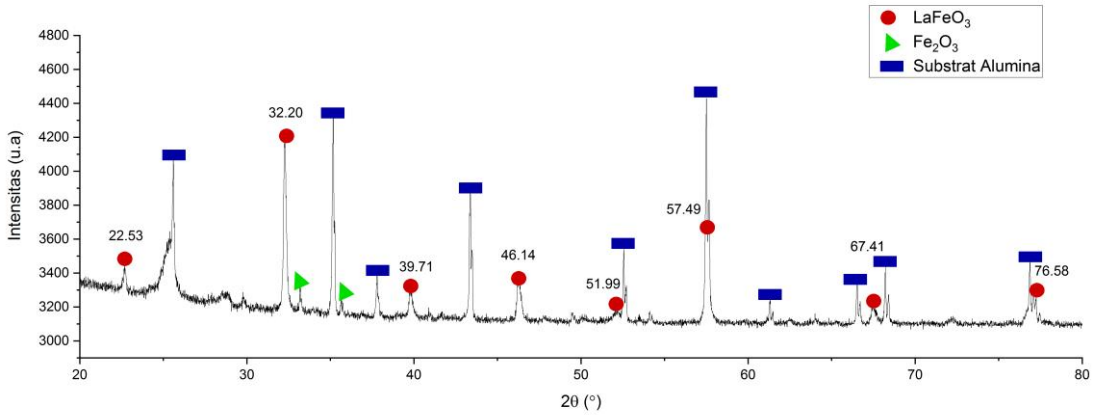

(a)

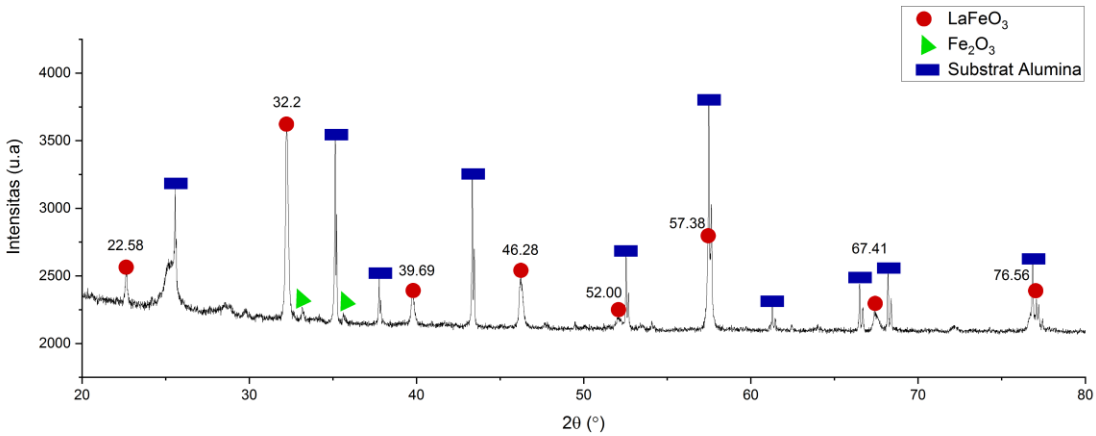

(b)

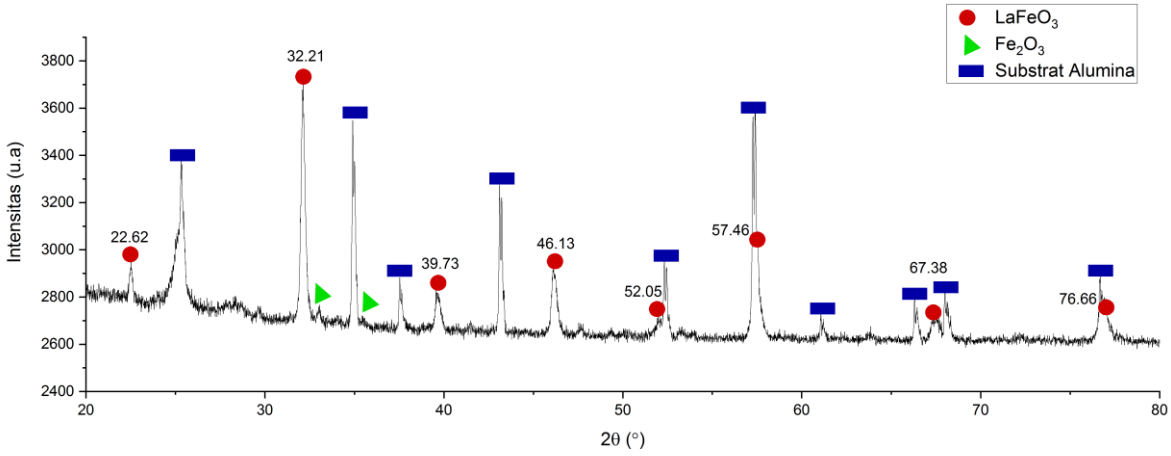

(c)

Figure 1. The Result of XRD Characterization of $LaFeO_3$ co-doping Gd and Co 2.5% with Gd (a) 0%, (b) 2.5%, and (c) 5%.

The reference from the Crystallography Open Database (COD) database no. 96-154-2033, shows that the LaFeO3 lattice parameter has the value of a = b = c = 3.9260Å. In comparison, they are not very different from the reference. This fact shows that the Gd^{3+} ion from Gd_2O_3 and Co^{2+}

ions from CoO have succeeded in substituting each La^{3+} ion from La_2O_3 and Fe^{3+} from Fe_2O_3. Gd^{3+} has an ionic radius of 1.07 Å, while La^{3+} has an ionic radius of 1.17 Å. Besides, Co^{2+} has an ionic radius of 0.79 Å, while Fe^{3+} has an ionic radius of 0.69 Å. Co^{2+} ion substitution on Fe^{3+} on each sample gives a LaFeO3 lattice parameter value greater than the reference. When Gd started to get in Gd^{3+}, which has an ionic radius smaller than La^{3+}, substituting La^{3+} ions, thus causing the lattice parameters to decrease as the Gd doping concentration is added [25].

The crystallite size decreases as the Gd doping concentration increases but expands at 2.5% Gd, which starts from 64,335 nm, 68,839 nm, to 65,752 nm. The crystallite size was calculated with the Debye-Scherrer Equation shown in Equation (1) [26].

Morphology Structure Characteristic

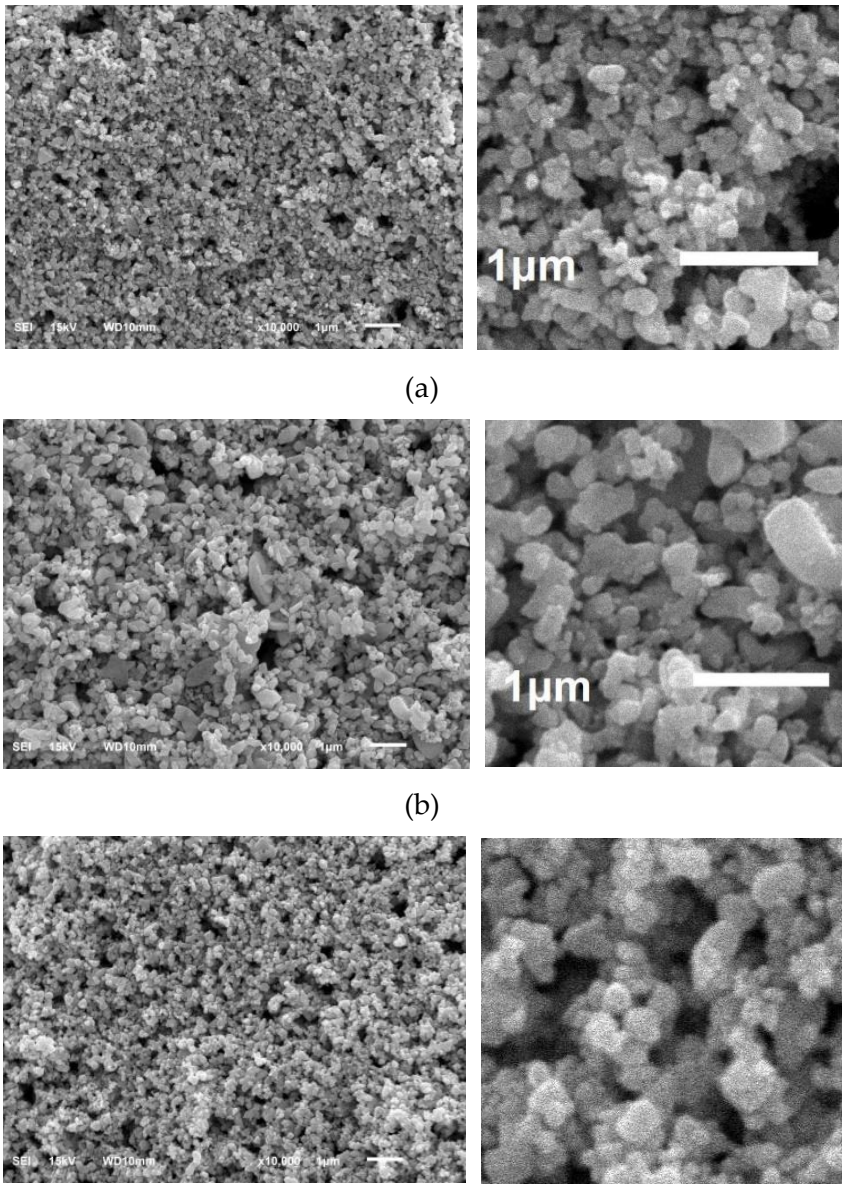

(a)

(b)

(c)

Figure 2. The Result of SEM Characterization of $LaFeO_3$ co-doping Gd and Co 2.5% with Gd (a) 0%, (b) 2.5%, and (c) 5%.

The results of the morphological structure characterization in the form of sample grain size

from the Scanning Electron Microscopy (SEM) test results are shown in Figure 2. The SEM test results on the thick film $LaFeO_3$ co-doping Co 2.5% with Gd 0%, 2.5%, and 5% indicate the average grain size in sequential order are 0.15 μm, 0.26 μm, and 0.16 μm which calculated using linear intercept method. Adding Gd 2.5% to the sample causes the average grain size to be larger than that of Gd 0%. The thick film $LaFeO_3$ co-doping Co 2.5% with Gd 5% has an average grain size smaller than Gd 2.5% but larger than Gd 0%. This phenomenon is in line with the crystallite size from the XRD test results, which shows that the crystallite size increases when 2.5% Gd is added. In addition, the grain sizes in this sample have a more uniform size with each other, compared to the other two samples.

Seeing the size of crystallite size in XRD results, with the same trend, the grain will increase in size after heat treatment and decrease after the next doping [5]. This fact might be because the doping didn't form very well with $LaFeO_3$, thus increasing the grain boundaries, so it didn't grow as much as the previous doping. This behavior happened in Neng Astri et al.' s research [24].

Electrical Properties Characteristic

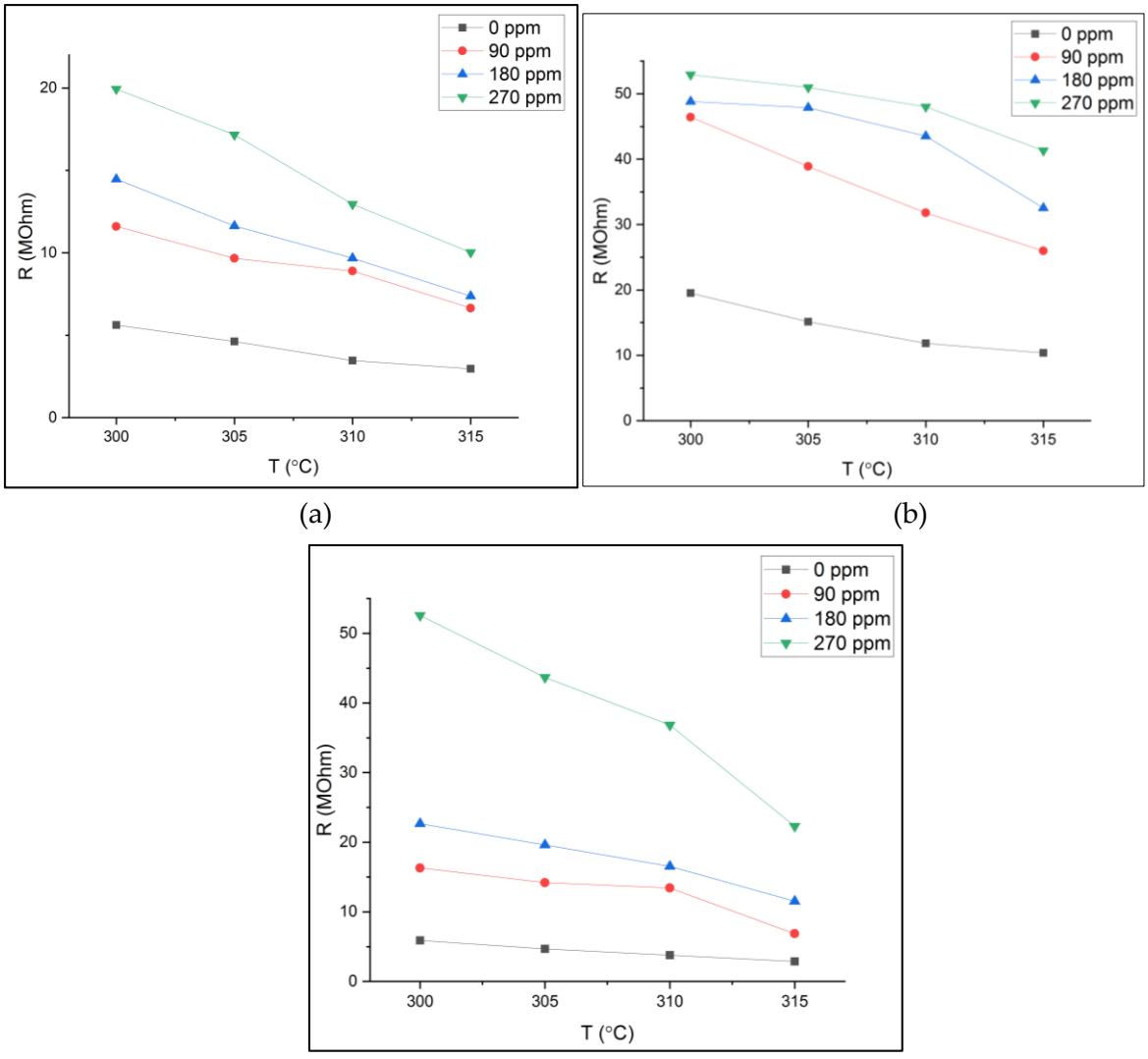

Figure 3. The effect of temperature on $LaFeO_3$ co-doping Gd and Co 2.5% thick film ceramic resistance with Gd (a) 0%, (b) 2.5%, and (c) 5%.

The results of the sample resistance measurement to temperature for each sample show that the resistance decreases as the temperature increases, as shown in Figure 3. The decrease in resistance value with increasing temperature is caused by ionized electrons from the valence band. The ionized electrons will leave holes in the valence band [27]. The higher the temperature, the more electrons are ionized, and the more holes are produced. The presence of this hole gives a decrease in the resistance value [28].

The results of the sample resistance measurement to temperature can also be used to find the sensitivity value for each sample [29] and determine the operating temperature of the gas sensor. This procedure is done using Equation (2), and the trend of temperature changes with sensitivity is shown in Figure 4.

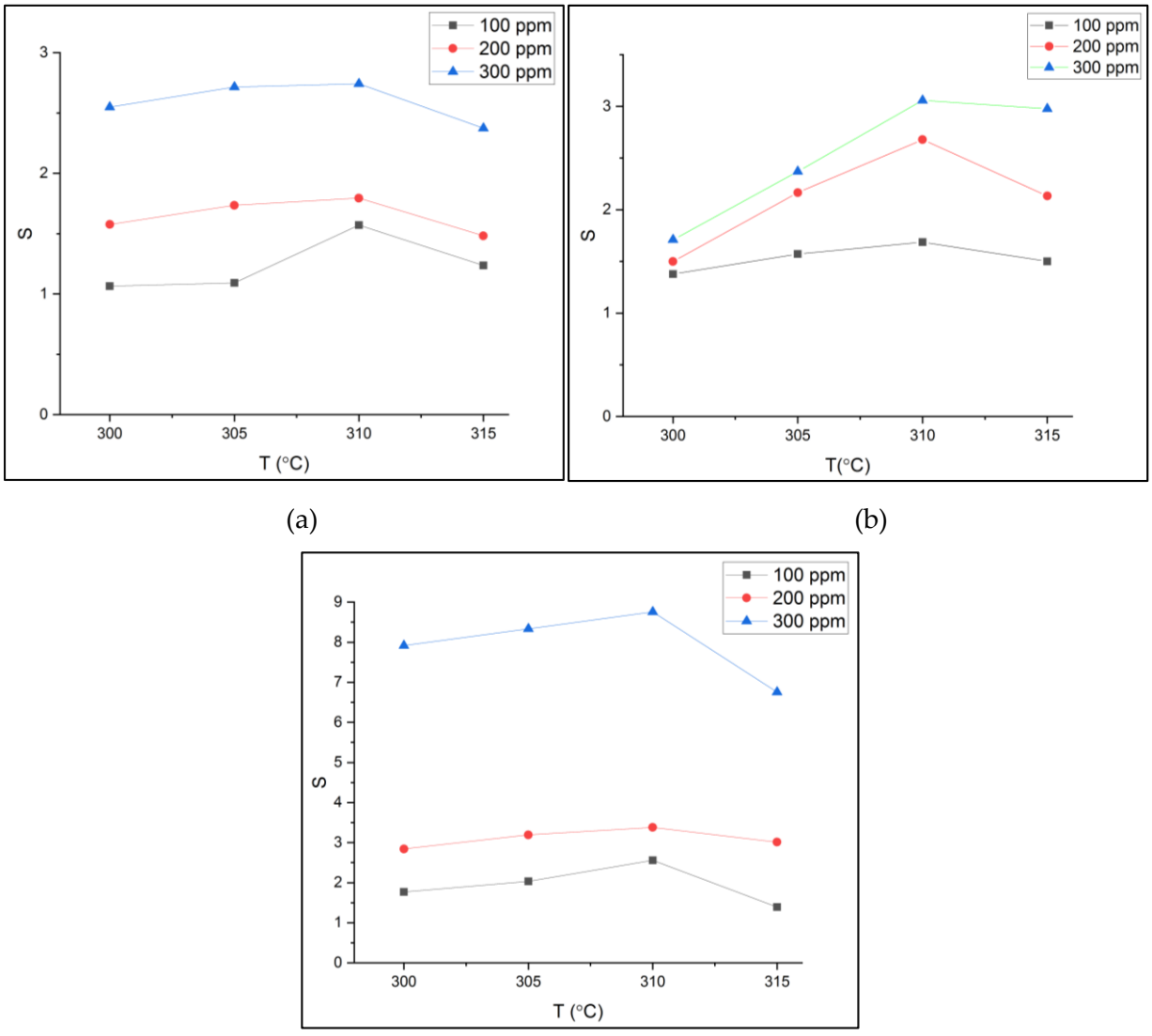

Figure 4. The effect of temperature on $LaFeO_3$ thick film ceramic sensitivity with (a) 0% Gd, (b) 2.5% Gd, and (c) 5% Gd.

Adding Gd doping to $LaFeO_3$ Co 2.5% affects the sensitivity value obtained. In addition, the concentration of gas that is used also has an influence on the sensitivity value obtained. The sensitivity increases with increasing Gd doping and the concentration of acetone gas being used

[19,30,31]. More detailed data is depicted in Table 1.

Table 1 The sensitivity and operating temperature of $LaFeO_3$ co-doping Co 2.5% with Gd 0%, Gd 2.5%, dan Gd 5% thick film ceramic.

Compounds	Operating Temperature (°C)	S		
		90 ppm	180 ppm	270 ppm
$LaFeO_3$ Co 2.5% Gd 0%	310°C	1.570199	1.794661	2.741911
$LaFeO_3$ Co 2.5% Gd 2.5%		1.686386	2.677766	3.057973
$LaFeO_3$ Co 2.5% Gd 5%		2.557392	3.379999	8.758197

The sensitivity value is obtained from the highest peak value on the sensitivity graph to the operating temperature, while the operating temperature is the temperature that provides the highest sensitivity [32]. Based on the data in Table 1, the operating temperature for the $LaFeO_3$ Co 2.5% thick film for each concentration of Gd has the same value, which is 310°C.

When the sensor surface is exposed to free air, the surface of the $LaFeO_3$ material adsorbs oxygen. Oxygen molecules attract electrons from the surface of $LaFeO_3$ to form adsorbed oxygen. When the temperature is increased, the adsorbed oxygen undergoes the following reaction [27,28]:

$$O_2(gas) \rightarrow O_2(ads) \tag{3}$$

$$O_2^-(ads) \rightarrow O^-(ads) \tag{4}$$

$$O^-(ads) \rightarrow O^{2-}(ads) \tag{5}$$

In this state, the electrons in the valence band gain thermal energy for ionization to the conduction band until they are captured by oxygen, leaving holes in the valence band. These holes' presence lowers the material's resistance [13]. The more oxygen is adsorbed, the more electrons are captured [33], and the more holes are formed.

When exposed to acetone gas, acetone gas will attract oxygen with the consequence that electrons in oxygen will be released on the material surface [34]. The possible reaction on the $LaFeO_3$ sensor can be explained by the equation (6):

$$\begin{aligned} &C_3H_6O_{(gas)} + 8O^n{}_{(ads)} \rightarrow \\ &3CO_{2(ads)} + 3H_2O_{(ads)} + 8ne^- \end{aligned} \tag{6}$$

The electrons that come will lose energy, so they will fall into the valence band where there is a hole [32]. Electrons will meet holes, and recombination occurs.

$$h^+ + e^- \rightarrow null \tag{7}$$

During recombination, electron-hole pairs are lost as charge carriers. The more electrons, the more recombination, and loss of holes as charge carriers. These phenomena cause the resistance value to be high [13,14]. This fact corresponds to the resistance value when the sample is exposed to gas [35]. Thus, from the measurement results of electrical properties, it is shown that $LaFeO_3$ co-doping Co 2.5% with Gd 0%, 2.5%, and 5% is a p-type semiconductor which is characterized by a smaller resistance value when without gas compared to when being exposed

to the gases [36].

As long as the temperature is continuously increased, the reaction of the adsorbed oxygen, both with the material's surface and with acetone gas, will continue to 310°C. When passing through it, the hole production will decrease drastically, which is indicated by reduced sensitivity. This result is because there are myriads of electron holes that recombine. [37].

From the crystal structure perspective, XRD results show that $LaFeO_3$ co-doping with CoO and Gd_2O_3 has been successfully achieved. In addition, from the sensitivity value, it is found that given doping concentration increases the sensitivity. This fact is supported by the SEM results showing grain sizes that are uniformly increasing to each other after doping was added. The grain sizes are distributed and more uniform, increasing the sensor's surface ratio, thus enabling the sensor to have high sensitivity [33].

However, compared with the previous references like by Hao et al. [15] and Zhang et al. [13], operating temperatures show a higher value. This fact is suspected from the synthesis process results until it becomes a paste that is not maximized. The addition of doping which is expected to lower the operating temperature has not been achieved. This result is supported by the results of the SEM test, which showed the morphological structure of sensors that have been made. However, for sensitivity, it has a more significant value compared to the study conducted by Zhang et al. [13]

This research could've done better with standardized experiment apparatus because this is actually the only limitation that this research faces. Besides, further studies can focus on the time response and higher range of doping that can be added to the sample, thus can make this research more appropriate scientifically to consider.

CONCLUSION

The synthesis and characterization by co-precipitation method on thick film ceramics $LaFeO_3$ co-doping Gd_2O_3 and CoO for acetone gas sensor applications have been carried out. The crystal structure of the $LaFeO_3$ thick film ceramics co-doping Co 2.5% with Gd 0%, Gd 2.5%, and Gd 5%, each of which has a cubic phase with the crystallite size decreasing as Gd doping concentration increases. The grain size increases when the sample is given Gd 2.5% and again decreases when given Gd 5%. The gas sensor with the addition of Gd 5% concentration has a higher sensitivity than the gas sensor with Gd 0% and 2.5% Gd. In addition, for each sample with the concentration of acetone gas tested, the operating temperature is shown to be 310°C. The high sensitivity after a couple of doping is achieved compared to the references. However, for the operating temperature, it shows a higher value when compared with the previous research reference. The crystallite size from XRD results and SEM results support it.

ACKNOWLEDGMENT

This work was financially supported by Penelitian Terapan Unggulan Perguruan Tinggi Kementerian Pendidikan, Kebudayaan, Riset, dan Teknologi Republik Indonesia Research grants Contract Number 1594/UN.40.LP/PT.01.03/2021.

AUTHOR CONTRIBUTIONS

Hendi Haryadi: Methodology, Formal Analysis, Investigation, and Writing - Review & Editing; Dani Gustaman Syarif: Conceptualization, Validation, Formal Analysis, and Supervision; and Endi Suhendi: Conceptualization, Formal Analysis, Writing - Original Draft

and Review & Editing.

DECLARATION OF COMPETING INTEREST

The authors declare that they have no known competing financial interests or personal relationships that could have appeared to influence the work reported in this paper.

REFERENCES

[1] Lin C, Xu W, Yao Q and Wang X. Chapter 9 - Nanotechnology on Toxic Gas Detection and Treatment. In Wang X and Chen X, *Novel Nanomaterials for Biomedical, Environmental and Energi Applications.* Amsterdam: Elsevier; 2019: 275-297. DOI: https://doi.org/10.1016/B978-0-12-814497-8.00009-6.

[2] Cai L, et al. Ultrasensitive Acetone Gas Sensor Can Distinguish the Diabetic State of People and Its High Performance Analysis by First-Principles Calculation. *Sensors and Actuators B: Chemical*. 2022; **351**: 130863. DOI: https://doi.org/10.1016/j.snb.2021.130863.

[3] Saruhan B, Fomekong RL, and Nahirniak S. Review: Influences of Semiconductor Metal Oxide Properties on Gas Sensing Characteristics. *Frontier in Sensors: Section Sensor Devices*. 2021; **2**: 657931. DOI: https://doi.org/10.3389/fsens.2021.657931.

[4] Kim K, Choi P, Itoh T, and Masuda Y. Catalyst-Free Highly Sensitive SnO_2 Nanosheet Gas Sensors for Parts per Billion-Level Detection of Acetone. *ACS Applied Materials and Interfaces*. 2020; **12**(46): 51637–51644. DOI: https://doi.org/10.1021/acsami.0c15273.

[5] Catauro M, Tranquillo E, Poggetto GD, Pasquali M, Dell'Era A and Ciprioti SV. Influence of the Heat Treatment on the Particles Size and on the Crystalline Phase of TiO_2 Synthesized by the Sol-Gel Method. *Materials*. 2018; **11**(12): 2364. DOI: https://doi.org/10.3390/ma11122364.

[6] Liang S, Li J, Wang F, Qin J, Lai X and Jiang X. Highly Sensitive Acetone Gas Sensor Based on Ultrafine α-Fe_2O_3 Nanoparticles. *Sensors and Actuators B: Chemical*. 2017; **238**: 923–927. DOI: https://doi.org/10.1016/j.snb.2016.06.144.

[7] Rong Q, et al. Enhanced Performance of an Acetone Gas Sensor Based on Ag-$LaFeO_3$ Molecular Imprinted Polymers and Carbon Nanotubes Composite. *Nanotechnology*. 2020; **31**: 405701. DOI: https://doi.org/10.1088/1361-6528/ab80f9.

[8] Cosandey F, Skandan G, and Singhal A. Materials and Processing Issues in Nanostructured Semiconductor Gas Sensors. *JOM-e*. 2000; **52**(10): 10. Available from: http://www.tms.org/pubs/journals/JOM/0010/Cosandey/Cosandey-0010.html.

[9] Suhendi E, Witra, Hasanah L, and Syarif DG. Characteristics of a Thick Film Ethanol Gas Sensor Made of Mechanically Treated $LaFeO_3$ Powder. *AIP Conference Proceedings.* 2017; **1848**: 050008. DOI: https://doi.org/10.1063/1.4983964.

[10] Sharma N, Kushwaha HS, Sharma SK, and Sachdev K. Fabrication of $LaFeO_3$ and rGO-$LaFeO_3$ Microspheres Based Gas Sensors for Detection of NO_2 and CO. *RSC Advances*. 2020; **10**(3): 1297–1308. DOI: https://doi.org/10.1039/C9RA09460A.

[11] Laysandra H and Triyono D. Effect of Fe_3O_4 Addition on Dielectric Properties of $LaFeO_3$ Nano-Crystalline Materials Synthesized by Sol-Gel Method. *IOP Conference Series: Materials Science and Engineering*. 2017; **188**: 012039. DOI: https://doi.org/10.1088/1742-6596/755/1/011001.

[12] Xu H, Xu J, Li H, Zhang W, Zhang Y, and Zhai Z. Highly Sensitive Ethanol and Acetone Gas Sensors with Reduced Working Temperature Based on Sr-Doped $BiFeO_3$

Nanomaterial. *Journal of Materials Research and Technology*. 2022; **17**: 1955–1963. DOI: https://doi.org/10.1016/j.jmrt.2022.01.137.

[13] Zhang L, Qin H, Song P, Hu J, and Jiang M. Electric Properties and Acetone-Sensing Characteristics of $La_{1-x}Pb_xFeO_3$ Perovskite System. *Materials Chemistry and Physics*. 2006; **98**(2-3): 358–362. DOI: https://doi.org/10.1016/j.matchemphys.2005.09.041.

[14] Ikram M, et al. Fabrication and Characterization of a High-Surface Area MoS_2@WS_2 Heterojunction for the Ultra-Sensitive NO_2 Detection at Room Temperature. *Journal of Materials Chemistry A*. 2019; **7**(24): 14602–14612. DOI: https://doi.org/10.1039/C9TA03452H.

[15] Hao P, Lin Z, Song P, Yang Z, and Wang Q. Hydrothermal Preparation and Acetone-sensing Properties of Ni-doped Porous $LaFeO_3$ Microspheres. *Journal of Material Science: Materials in Electronics*. 2019; **31**: 6679-6689. DOI: https://doi.org/10.1007/s10854-020-03224-x.

[16] Sarf F. Metal Oxide Gas Sensors by Nanostructures In Khan SB, Asiri AM, and Akhtar K, *Gas Sensors*. London: Intechopen; 2019. DOI: https://doi.org/10.5772/intechopen.88858.

[17] Jabalah S, Dahman H, Neri G, and El Mir L. Effect of Al and Mg Co-Doping on the Microstructural and Gas-Sensing Characteristics of ZnO Nanoparticles. *Journal of Inorganic and Organometallic Polymers and Materials*. 2020; **31**(4): 1653-1667. DOI: https://doi.org/10.1007/s10904-020-01796-z.

[18] Salah LM, Haroun M, and Rashad MM. Structural, Magnetic, and Electrical Properties of Gd-Substituted $LaFeO_3$ Prepared by co-Precipitation Method. *Journal of the Australian Ceramic Society*. 2017; **54**(2): 357–368. DOI: https://doi.org/10.1007/s41779-017-0160-5.

[19] Zahmouli N, et al. High Performance Gd-Doped γ-Fe_2O_3 Based Acetone Sensor. *Materials Science in Semiconductor Processing*. 2020; **116**: 105154. DOI: https://doi.org/10.1016/j.mssp.2020.105154.

[20] Rani TD, Ramamurthi K, and Leela S. Structural and Optical Properties of Gd Doped ZnO Thin Films by Spray Pyrolysis Technique. *AIP Conference Proceedings*. 2019; **2117**(1): 020003. DOI: https://doi.org/10.1063/1.5114583.

[21] Zhang X, et al. Designed Synthesis of Co-Doped Sponge-like In_2O_3 for Highly Sensitive Detection of Acetone Gas. *CrystEngComm*. 2019; **21**: 1876–1885. DOI: https://doi.org/10.1039/C8CE02058B.

[22] Amanda ZL. *Pengaruh co-Doping ZnO dan CaO terhadap Karakteristik Keramik Film Tebal $LaFeO_3$ untuk Aplikasi Sensor Gas Etanol*. Undergraduate Thesis. Bandung: Universitas Pendidikan Indonesia; 2019. Available from: http://repository.upi.edu/41248/.

[23] Fioravanti A, et al. Growth Mechanisms of ZnO Micro-Nanomorphologies and Their Role in Enhancing Gas Sensing Properties. *Sensors*. 2021; **21**(4): 1331. DOI: https://doi.org/10.3390/s21041331.

[24] Suhendi E, Lidiawati NA, Setiawan A, and Syarif DG. Synthesis and Characterization of Al_2O_3-Doped $LaFeO_3$ Thick Film Ceramics for Ethanol Gas Sensing Application. *Oriental Journal of Chemistry*. 2019; **35**(1): 283–288. DOI: https://doi.org/10.13005/ojc/350134.

[25] Suhendi E, Ulhakim MT, Setiawan A, and Syarif DG. The Effect of SrO Doping on $LaFeO_3$ using Yarosite Extraction Based Ethanol Gas Sensors Performance Fabricated by Coprecipitation Method. *International Journal of Nanoelectronics and Materials*. 2019; **12**(2): 185–192. Available from: http://dspace.unimap.edu.my/xmlui/handle/123456789/59931.

[26] Al-Bataineh QM, et al. Synthesis, Crystallography, Microstructure, Crystal Defects,

Optical and Optoelectronic Properties of ZnO:CeO_2 Mixed Oxide Thin Films. *Photonics*. 2020; **7**(4): 112. DOI: https://doi.org/10.3390/photonics7040112.

[27] Barsoum M. *Fundamentals of Ceramics*. Philadelphia, PA : Institute of Physics Pub; 2003.

[28] Jiang H and Shen Y-C. Ionization Potentials of Semiconductors from First-Principles. *The Journal of Chemical Physics*. 2013; **139**(16): 164114. DOI: https://doi.org/10.1063/1.4826321.

[29] Hosseinzadeh H, Tohidi G, Movahedi F, and Hassannayebi E. Optimization and Modeling of Zn_2SnO_4 Sensitivity as Gas Sensor for Detection Benzene in the Air by Using the Response Surface Methodology. *Journal of Saudi Chemical Society*. 2021; **25**(12): 101371. DOI: https://doi.org/10.1016/j.jscs.2021.101371.

[30] Kasirajan K, Chandrasekar LB, Maheswari S, Karunakaran M, and Sundaram PS. A Comparative Study of Different Rare-Earth (Gd, Nd, and Sm) Metals Doped ZnO Thin Films and Its Room Temperature Ammonia Gas Sensor Activity: Synthesis, Characterization, and Investigation on the Impact of Dopant. *Optical Materials*. 2021; **121**: 111554. DOI: https://doi.org/10.1016/j.optmat.2021.111554.

[31] Rao SK, et al. Unraveling the Potential of Gd Doping on Mullite $Bi_2Fe_4O_9$ for Fiber Optic Ethanol Gas Detection at Room Temperature. *Materials Chemistry and Physics*. 2022; **278**: 125646. DOI: https://doi.org/10.1016/j.matchemphys.2021.125646.

[32] Plecenik T, et al. Fast Highly-Sensitive Room-Temperature Semiconductor Gas Sensor Based on the Nanoscale Pt–TiO_2–Pt Sandwich. *Sensors and Actuators B: Chemical*. 2015; **207**(A): 351-361. DOI: https://doi.org/10.1016/j.snb.2014.10.003.

[33] Chen Y, Qin H, Wang X, Li L, and Hu J. Acetone Sensing Properties and Mechanism of Nano-$LaFeO_3$ Thick-Films. *Sensors and Actuators B: Chemical*. 2016; **235**: 56–66. DOI: https://doi.org/10.1016/j.snb.2016.05.059.

[34] Moumen A, Kumarage GCW, and Comini E. P-Type Metal Oxide Semiconductor Thin Films: Synthesis and Chemical Sensor Applications. *Sensors*. 2022; **22**(4): 1359. DOI: https://doi.org/10.3390/s22041359.

[35] Raju P and Li Q. Review—Semiconductor Materials and Devices for Gas Sensors. *Journal of The Electrochemical Society*. 2022; **169**: 057518. DOI: https://doi.org/10.1149/1945-7111/ac6e0a.

[36] Murade P, Sangawar PS, Chaudhari GN, Kapse VD, and Bajpeyee AU. Acetone Gas-Sensing Performance of Sr-Doped Nanostructured $LaFeO_3$ Semiconductor Prepared by Citrate Sol-gel Route. *Current Applied Physics*. 2011; **11**(3): 451–456. DOI: https://doi.org/10.1016/j.cap.2010.08.020.

[37] Fine GF, Cavanagh LM, Afonja A, and Binions R. Metal Oxide Semi-Conductor Gas Sensors in Environmental Monitoring. *Sensors (Basel)*. 2010; **10**(6): 5469-5502. DOI: https://doi.org/10.3390/s100605469.